BMC Cancer

RESEARCH

Open Access

Pretreatment plasma sCD14 as a prognostic indicator in advanced non-small cell lung cancer patients undergoing immunotherapy

Liyuan Dai[1], Liling Huang[1], Lin Li[2], Le Tang[1], Jiarui Yao[1], Yuankai Shi[1*] and Xiaohong Han[3*]

Abstract

Background This study aims to evaluate cytokines as a prognostic biomarker in patients with advanced non-small cell lung cancer (aNSCLC) undergoing immunotherapy.

Methods A comprehensive analysis was conducted to assess the prognostic significance of sCD14 and other cytokines in aNSCLC patients receiving immune checkpoint inhibitors (ICIs) using flow fluorescence. A discovery cohort ($n=42$) was used to evaluate the differential expression of 41 cytokines between durable clinical benefit (DCB) and no durable benefit (NDB) groups in Cancer Hospital, Chinese Academy of Medical Sciences (CHCAMS). The prognostic value was further validated in multiple independent cohorts, including plasma protein measurements ($n=109$), multiplex immunofluorescence (mIF) ($n=22$), and messenger RNA datasets ($n=403$) of NSCLC in CHCAMS.

Results In the discovery cohort, 7 cytokines (CD14, CCL27, IL-17 A, EGF, TNFR1, GFAP, CHI3L1) exhibited differential expression between the DCB and NDB groups. Among these, CD14, CCL27, IL-17 A, and TNFR1 were significantly elevated in the DCB group, while EGF, CHI3L1, and CCL5 were higher in the NDB group. CD14 showed a high area under the curve (AUC = 0.84) for predicting clinical benefit. Functional enrichment analysis indicated that these cytokines are involved in key immune pathways, including the inflammatory response and MAPK signaling. Univariate COX for progression-free survival (PFS) analysis demonstrated prognostic value for CD14 ($p<0.001$, $HR=0.054$ [0.014–0.219]), CCL27 ($p<0.001$, $HR=0.054$ [0.015–0.196]), IL-17 A ($p<0.001$, $HR=0.110$ [0.041–0.298]), and CCL5 ($p<0.05$, $HR=2.387$ [1.023–5.570]). Validation in the CHCAMS cohort confirmed that CD14 expression, measured via mIF, was a predictor of PFS ($p<0.05$). Furthermore, high *CD14* expression was consistently associated with superior PFS across multiple external datasets (GSE126044, GSE135222, GSE136961, and GSE218989). *CD14* expression was found to be elevated in various normal tissue types, particularly in lung adenocarcinoma and lung squamous cell carcinoma, compared to tumors, indicating its potential role in immune surveillance.

Conclusion sCD14 is a promising prognostic biomarker for aNSCLC patients undergoing immunotherapy. Elevated plasma sCD14 levels are associated with improved PFS and a favorable immune response.

Keywords sCD14, Immunotherapy, Prognostic biomarker, Non-small cell lung cancer

*Correspondence:
Yuankai Shi
syuankai@cicams.ac.cn
Xiaohong Han
hanxiaohong@pumch.cn

Full list of author information is available at the end of the article

Introduction

Advanced non-small cell lung cancer (aNSCLC) is a leading cause of cancer-related mortality globally, with a significant portion of patients presenting with advanced or metastatic disease at diagnosis [1, 2]. Despite recent advances in treatment, particularly with the advent of immune checkpoint inhibitors (ICIs), the response to immunotherapy in aNSCLC patients remains highly variable, with non-responders constituting three-quarters of NSCLC patients under immunotherapy [3, 4], necessitating the identification of reliable prognostic biomarkers to guide clinical decisions and optimize therapeutic outcomes.

Combining ICIs with chemotherapy has demonstrated synergistic effects, resulting in substantial improvements in overall response rates (ranging from 28.4 to 63.5%) and survival outcomes [5]. However, currently available prognostic biomarkers such as programmed death ligand-1 (PD-L1) expression, tumor mutational burden, and microsatellite instability-high/deficient mismatch repair show modest predictive power [6, 7]. In NSCLC treated with ICIs, previous studies have identified various biomarkers for monitoring, including peripheral blood circulating tumor DNA [8, 9], neutrophil-to-lymphocyte ratio [10], C-reactive protein [11], interleukin-6 (IL-6) [12], interleukin-8 (IL-8) [13, 14], CXCL8, CXCL10 [15], and autoantibody (AAb) panels associated with autoimmune diseases (antinuclear, thyroglobulin, thyroid peroxidase AAbs) [16]. Additionally, specific AAbs (such as lgM-RF [17], NY-ESO-1, XAGE1 [18], p53, BRCA2, HUD, and TRIM21 AAbs [19]), homeobox protein SIX2 AAb [20], lgG4 AAb targeting programmed cell death protein 1 [21], and lgG AAb targeting myc associated factor X [22] have also been investigated.

Plasma cytokines have emerged as promising predictive biomarkers in patients receiving immunotherapy due to their critical role in modulating the immune response. Cytokine profiles can reflect the inflammatory and immunoregulatory environment, which is essential for determining the efficacy of ICIs. Several studies [12, 13, 23–25] have demonstrated that elevated levels of specific cytokines, such as IL-6 and IL-8, are associated with treatment response in patients undergoing ICIs therapy. Among them, IL-8 exerts its effects by binding to chemokine receptors CXCR1 and CXCR2, thereby modulating inflammatory responses, stimulating angiogenesis, and promoting tumor cell proliferation [13, 23]. Changes in serum IL-8 levels before and after ICIs treatment have been shown to predict and monitor therapeutic efficacy in patients with aNSCLC, with higher IL-8 levels correlating with poorer prognosis [13, 24, 25]. Furthermore, Keegan et al. [12] found that a dynamic decrease in IL-6 levels in NSCLC patients was positively associated with a longer median progression-free survival. However, prognostic biomarkers for immunotherapy remain to be further explored.

The present study aimed to investigate the cytokines in pretreatment plasma samples from aNSCLC patients undergoing chemoimmunotherapy. Our comprehensive findings contribute to the identification of predictive cytokines and provide valuable insights into the underlying mechanisms of resistance to chemoimmunotherapy. These results have the potential to improve patient stratification and guide personalized treatment decisions, ultimately enhancing outcomes for aNSCLC patients.

Methods

Study populations and sample collection

Between 2016 and 2022, a total of 151 pretreatment plasma samples and 22 formalin-fixed paraffin-embedded (FFPE) samples were collected from 173 patients with aNSCLC who received ICIs therapy (nivolumab, pembrolizumab, sintilimab, triplimab, camrelizumab, or tirellizumab) at the Cancer Hospital, Chinese Academy of Medical Sciences (CHCAMS). Plasma samples were collected in the morning on the day before patients received their immunotherapy, using ethylenediaminetetraacetic acid, centrifuged at 3000 rpm at 4 °C for 10 min, and stored in 2 ml conical tubes at -80 °C until the cytokine detection assays. FFPE samples were stored at room temperature. The personnel conducting cytokine detection were blinded to the patients' immune response outcomes.

The inclusion criteria for patient selection were as follows: (1) biopsy-confirmed diagnosis of NSCLC with stage III or IV disease and complete clinical follow-up data; (2) treatment with ICIs therapy; and (3) administration of ICIs as first-line or later-line therapy for at least two cycles. Patients were excluded if they met any of the following conditions: (1) concurrent diagnosis of other cancers; (2) presence of non-primary lung tumors; (3) diagnosis of concomitant autoimmune diseases (4) use of other immunosuppressive agents (e.g., steroid medication); or (5) presence of metabolic-related diseases such as diabetes, liver dysfunction, or kidney dysfunction. The efficacy of immunotherapy was evaluated using the Response Evaluation Criteria in Solid Tumours (RECIST) version 1.1. Treatment response was initially assessed by clinicians from the CHCAMS and subsequently reviewed by Dr. Huang for consistency. Patients were categorized as having a durable clinical benefit (DCB) if they achieved complete remission (CR), partial remission (PR), or stable disease (SD) after six months of ICI treatment, and as having a non-durable clinical

benefit (NDB) if they experienced disease progression (PD). This study was approved by the Ethics Committee of the National Cancer Center/National Clinical Research Center for Cancer/Cancer Hospital, Chinese Academy of Medical Sciences & Peking Union Medical College (No. 23/262–4004 and No.22/486–3688) and was conducted in accordance with the principles of the Declaration of Helsinki. All clinical characteristics of the multiple immunofluorescence (mIF) cohort and cytokine cohorts were summarized in Table S1.

Cytokine detection and analysis

In the discovery cohort, the quantitative detection of 41 cytokines in the plasma of aNSCLC patients was performed using flow fluorescence. The cytokines measured included CHI3L1, IFN-γ, IL-2, IL-5, IL-6, IL-8, IL-10, CD274, IL-17 A, IL-2R, B7-1, CCL11, CCL27, CCL5, CD105, CD14, FLT3L, GM-CSF, HE4, ICAM-1, IFN-α, IL-1β, IL-33, IL-7, IL-12P70, IL-15, LEPTIN, LGALS3, CCL7, CCL3, CCL4, CCL20, TNF-α, IL-4, TNFR1, CD40, CD69, GFAP, IL-1α, EGF, and VEGF. The procedure involved preparing the samples and the concentrated wash solution (RM59404, ABplex Human 41) according to the protocol. Subsequently, 50 µl/well of standards (220, 110, 55, 27.5, 13.75, and 6.87 ng/mL) or samples and 5 µl/well of microsphere suspension (RM59557, ABplex Human 41) were added to the microplate. The plate was covered with sealing film, thoroughly mixed, and incubated at 37 °C in the dark for 60 min at 1200 rpm in a constant temperature incubator. After incubation, the reaction plate was placed on a magnetic plate for magnetic separation for 2 min. The sealing film was removed, and while still on the magnetic plate, the supernatant was discarded, and any residual liquid was absorbed with blotting paper. Next, 100 µl/well of wash solution was added, mixed in a constant temperature incubator at 1200 rpm for 1 min, placed on a magnetic plate for 2 min, and the supernatant discarded again with blotting paper used to remove any residual liquid. Then, 50 µl/well of biotinylated antibody (RM59558, ABplex Human 41) was added, the plate was covered with sealing film, and incubated at 37 °C in the dark for 30 min at 1200 rpm in a constant temperature incubator. Following this, 50 µl/well of streptavidin-conjugated phycoerythrin (RM59400, ABplex Human 41) was added, the plate was again covered with sealing film, and incubated at 37 °C in the dark for 15 min at 1200 rpm in a constant temperature incubator. After incubation, the reaction plate was removed from the magnetic plate, 70 µl/well of wash solution was added, mixed thoroughly, and the detection was performed. The detection of eight cytokines in the validation cohort, including CHI3L1, IL-17 A, CCL5, CD14, GFAP, EGF, CCL27, and TNFR1, followed the same protocol as described above.

Calculate the mean absorbance for each set of duplicate standards, controls, and samples, and subtract the average optical density of the zero standard. Plot the standard curve on log-log graph paper, with standard concentration on the x-axis and absorbance on the y-axis, and draw the best-fit straight line through the standard points. For samples that have been diluted, multiply the concentration obtained from the standard curve by the dilution factor to determine the actual concentration of the target protein.

Multiple immunofluorescence

FFPE tissue sections, 4–5 µm in thickness, were prepared and subjected to dewaxing and rehydration. Antigen retrieval was performed, followed by blocking of endogenous peroxidase activity with an antibody blocking solution. Sequential immunostaining was carried out for each target antigen, starting with primary antibodies: rabbit anti-human CD14 (ab133335, dilution 1:5000, Abcam) and mouse anti-human pan-cytokeratin (GB122053, dilution 1:2000, Servicebio). This was followed by incubation with secondary antibodies: HRP-labeled goat anti-rabbit IgG (GB23303, dilution 1:500, Servicebio) for CD14, and HRP-labeled goat anti-mouse IgG (GB23301, dilution 1:500, Servicebio) for pan-cytokeratin. Tyramide signal amplification (TSA) was used, with subsequent microwave treatment to remove the TSA-antibody complex, allowing for additional rounds of antibody labeling. iF440-Tyramide (G1250, dilution 1:500, Servicebio) was used for CD14, and iF647-Tyramide (G1232, dilution 1:500, Servicebio) for pan-cytokeratin. After immunostaining, cell nuclei were counterstained with 4',6-diamidino-2-phenylindole (DAPI), and the slides were coverslipped for scanning. Microscopy (ECLIPSE C1, Nikon) and scanning (Pannoramic MIDI, 3DHISTECH) were employed for result interpretation, while quantification of the number and percentage of positive cells was performed using CaseViewer 2.4 (3DHISTECH) and ImageJ software. Two experienced pathologists independently reviewed all results.

Lymphocyte subsets and lymphocyte count detection

Laboratory tests were conducted to analyze the percentages and counts of $CD3^+$ T (total T) cells, $CD3^+CD4^+$ T (Th) cells, $CD3^+CD8^+$ T (Ts) cells, $CD3^-CD16^+CD56^+$ (NK) cells, and $CD3^-CD19^+$ (B) cells were analyzed by Flow Cytometry using the BD FACS Calibur. This analysis was performed on a subgroup of 72 aNSCLC patients, including 29 patients in the discovery cohort and 43 in the validation cohort. For peripheral lymphocyte subset analysis, 3 mL of

whole blood was collected from each patient when available, and flow cytometry was conducted. The monoclonal antibodies used in the staining panel included CD3 FITC, CD4 PE, CD8 PE, CD19 APC, CD45RA FITC, and $CD16^{+}CD56$ PE (BD FACS Calibur). The percentage of each lymphocyte subset, including total T cells, helper T cells, cytotoxic T cells, NK cells, and B cells, was recorded for each individual.

Bulk-RNA sequencing by GEO datasets analysis

Immunotherapy datasets from Gene Expression Omnibus data base (GEO) (https://www.ncbi.nlm.nih.gov/geo/) database, including GSE126044 [26] (platform GPL16791, $n = 16$ NSCLC), GSE135222 [27] (GPL16791, $n = 27$ NSCLC), and GSE218989 [28] ($n = 339$ NSCLC) were annotated and utilized for immunotherapy prediction analysis. The raw data were subjected to rigorous quality control using the 'Affy'

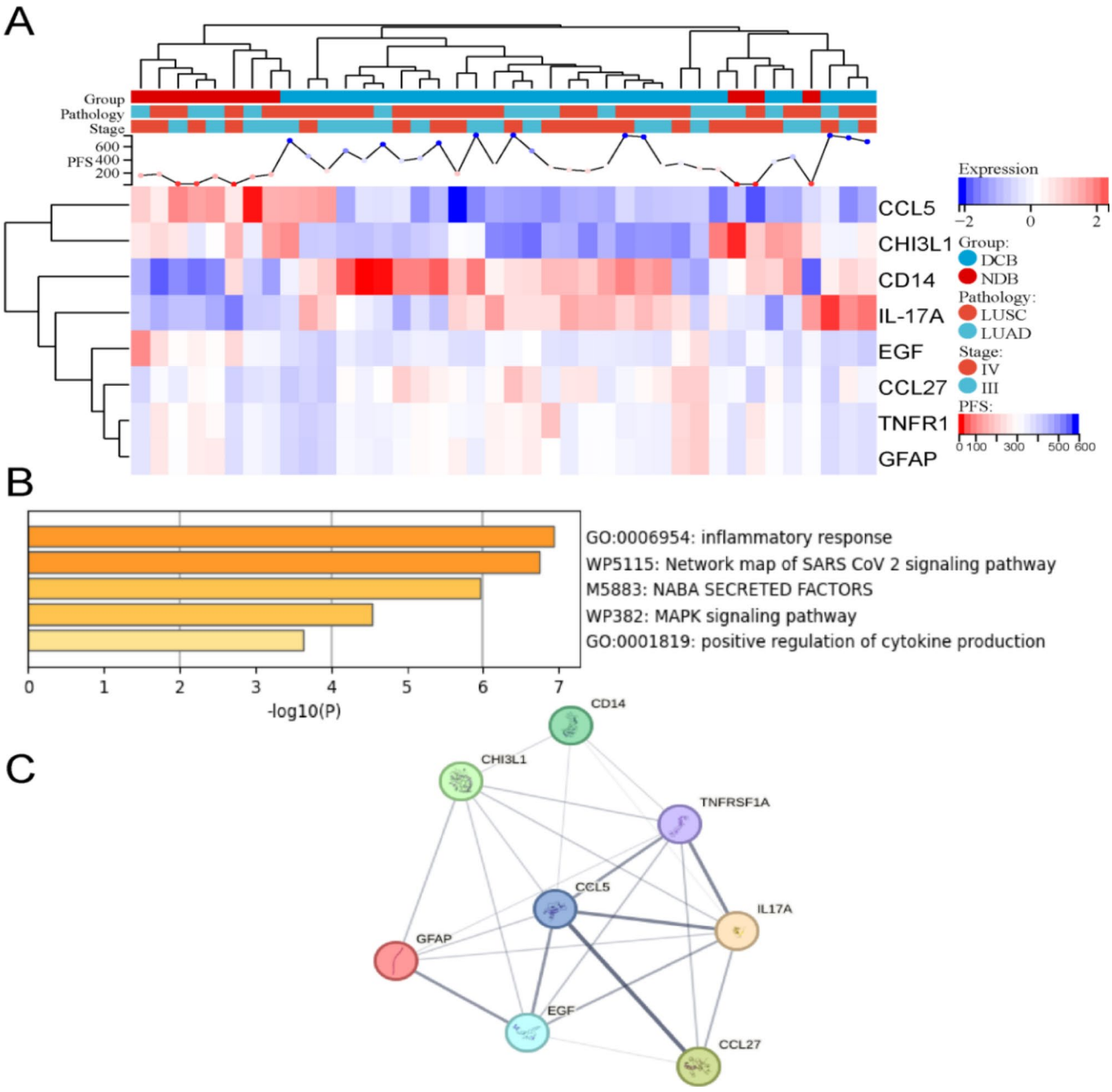

Fig. 1 Differential cytokines between NDB and DCB in the aNSCLC discovery cohort ($n = 42$). (**A**) Heatmap depicts the eight differential cytokines in NDB versus DCB patients with aNSCLC. (**B**) Functional enrichment analysis of the eight cytokines identified. (**C**) Protein-protein interaction network for the eight differential cytokines. (Abbreviation: NDB: non-durable clinical benefit; DCB: durable clinical benefit; aNSCLC: advanced non-small cell lung cancer; LUAD: lung adenocarcinoma; LUSC; lung squamous cell carcinoma)

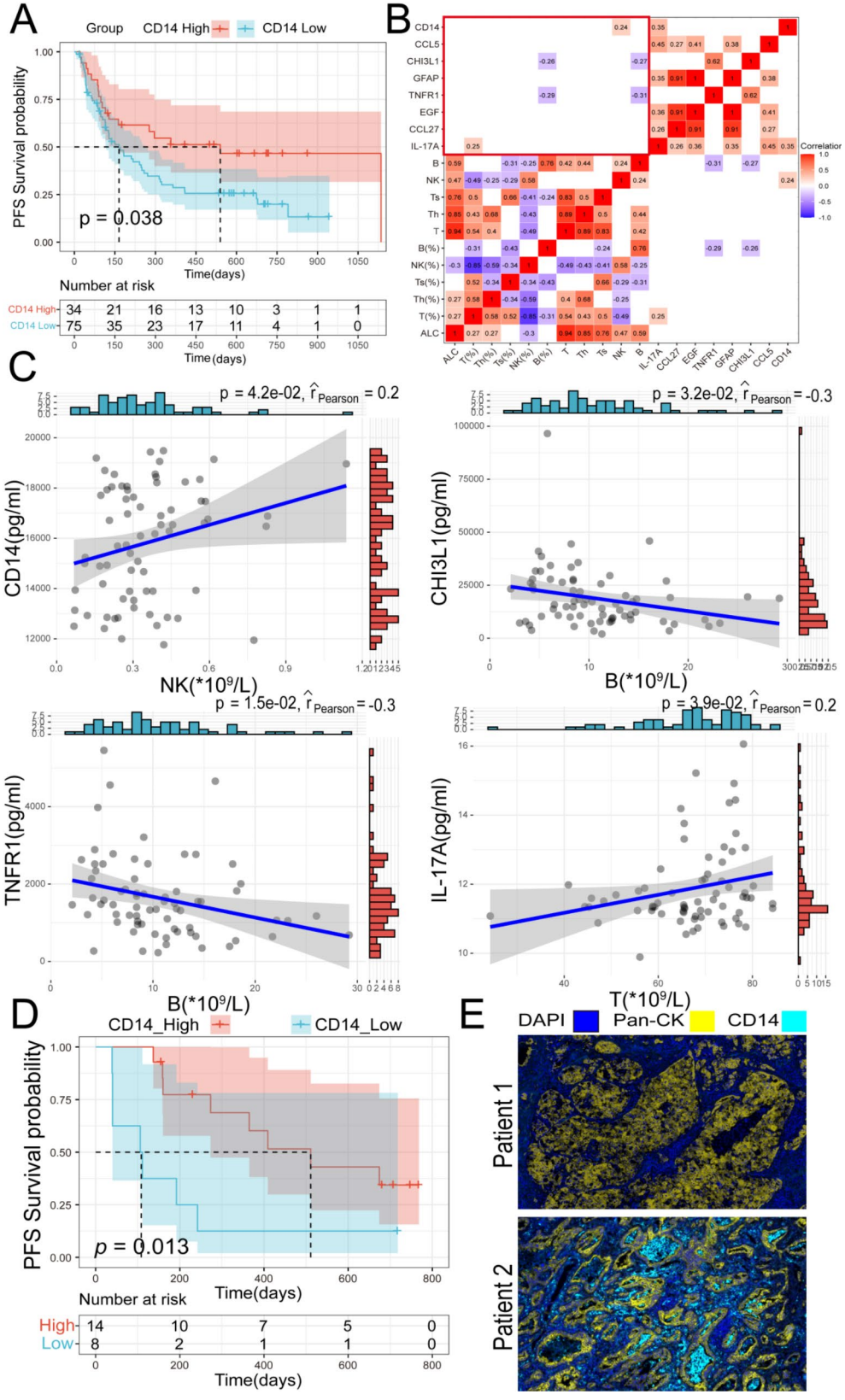

Fig. 2 (See legend on next page.)

(See figure on previous page.)

Fig. 2 Validation of the prognostic value of eight cytokines in the aNSCLC validation cohort ($n = 109$) and performance of CD14 in predicting PFS in the dynamic cohort and mIF cohort ($n = 21$). (**A**) Kaplan-Meier curve for PFS based on CD14 expression. (**B-C**) Correlation between the eight cytokines and lymphocyte subsets, including $CD3^+$ T (total T) cells, $CD3^+CD4^+$ T (Th) cells, $CD3^+CD8^+$ T (Ts) cells, $CD3^-CD16^+CD56^+$ (NK) cells, and $CD3^-CD19^+$ (B) cells. (**D**) Kaplan-Meier analysis of PFS based on CD14 intensity. (**E**) Representative mIF staining of DAPI, CD14, and pan Cytokeratin in patient #1 with short PFS (106 days) and patient #2 with long PFS (511 days). (Abbreviation: aNSCLC: advanced non-small cell lung cancer; PFS: progression free survival; mIF: multiple immunofluorescence; Mann-Whitney test was performed between groups)

package in R, which involved computing average values for multiple probes corresponding to a single gene. Clinical characteristics are summarized in Table S3. For the NSCLC immunotherapy datasets (GSE126044 and GSE135222), batch effects were corrected using 'combat' from the 'sva' package. The integrated dataset was labeled as NSCLC_ICIs. For GSE136961 [29] dataset, Kaplan-Meier curve for progression free survival (PFS) based on CD14 expression was performed in the Biomarker Exploration of Solid Tumors (BEST) (https://rookieutopia.hiplot.com.cn/app_direct/BEST/) website.

Statistical analysis

All statistical analyses were performed using the R version 4.3.1 software, Sangerbox plot (http://www.sangerbox.com), and Hiplot website (https://hiplot.com.cn/home/index.html). Mann-Whitney U tests were used to compare the DCB and NDB groups. Sensitivity, specificity, and receiver operating characteristic (ROC) curves were calculated with the 'pROC' and 'ROCR' packages. The 'maxstat' package in R was employed to determine the optimal cutoff values for high- and low-expression groups in both the training and validation phases. A significance level of $p < 0.05$ (two-tailed) was considered statistically significant for all analyses.

Results

Study design

The study consisted of two phases: discovery and validation. The clinical characteristics of the discovery and validation cohorts, including age, gender, histological type, stage, and line of therapy, have been matched ($P > 0.05$) (Table S1). In addition, the clinical characteristics of the NDB and GCB groups have also been matched ($P > 0.05$) (Table S2). In the discovery phase, plasma samples from a cohort of aNSCLC patients ($n = 42$) were collected prior to immunotherapy treatment. A total of 41 cytokines were analyzed to identify those with differential expression between patients with DCB and those with NDB. Eight cytokines, including sCD14, were found to have different levels between the two groups. In the validation phase ($n = 109$), the prognostic value of these eight cytokines was further assessed in an independent cohort. Given the critical role of the PD-L1 biomarker in lung cancer immunotherapy, we analyzed 21 patients with available PD-L1 data from both the discovery and validation cohorts to assess the independent predictive value of sCD14. The study utilized mIF ($n = 22$) and gene expression datasets (GSE126044, GSE135222, GSE136961, and GSE218989) to validate the findings. The correlation between sCD14 and lymphocyte subsets was also analyzed. The study included both messenger RNA (mRNA) and protein-level analyses to confirm the expression patterns of CD14 in normal versus tumor samples across various cancer types.

Discovery and validation cohorts of prognostic cytokines

Standard curve was shown in the Figure S1A. Among the 41 cytokines analyzed, 8 cytokines (CD14, CCL27, IL-17 A, EGF, TNFR1, GFAP, CHI3L1, CCL5) exhibited differential expression between the DCB ($n = 30$) and NDB ($n = 12$) groups in the discovery cohort (Fig. 1A, Table S4). CD14, CCL27, IL-17 A, TNFR1, and GFAP were elevated in the DCB group, whereas EGF, CHI3L1, and CCL5 were higher in the NDB group (Figure S1B, Table S4). The AUCs for CCL27, IL-17 A, EGF, TNFR1, GFAP, CHI3L1, CCL5, and CD14 were 0.875, 0.865, 0.755, 0.705, 0.726, 0.749, 0.749, and 0.84, respectively (Figure S1C, Table S5). Functional enrichment analysis revealed that these eight cytokines are involved in inflammatory response, the SARS-CoV-2 signaling pathway, the MAPK signaling pathway, and positive regulation of cytokine production (Fig. 1B). The protein-protein network analysis indicated strong interactions among these cytokines (Fig. 1C). Univariate analysis of progression-free survival demonstrated that CCL27 ($p < 0.001$, $HR = 0.054$ [0.015–0.196]), IL-17 A ($p < 0.001$, $HR = 0.110$ [0.041–0.298]), CD14 ($p < 0.001$, $HR = 0.054$ [0.014–0.219]), and CCL5 ($p < 0.05$, $HR = 2.387$ [1.023–5.570]) have prognostic value (Figure S1D).

Based on the results from the discovery cohort, eight cytokines were selected for validation. The standard curve for these eight cytokines was shown in the Figure S1E. Among these cytokines, CD14 demonstrated prognostic value for predicting PFS in aNSCLC patients receiving immunotherapy (Fig. 2A). Analysis of the correlation between these eight cytokines and lymphocyte subsets ($n = 70$) revealed that CD14 was positively correlated with NK cell counts ($p < 0.05$, $r = 0.24$). Conversely, CHI3L1 and TNFR1 were negatively correlated with both the percentage

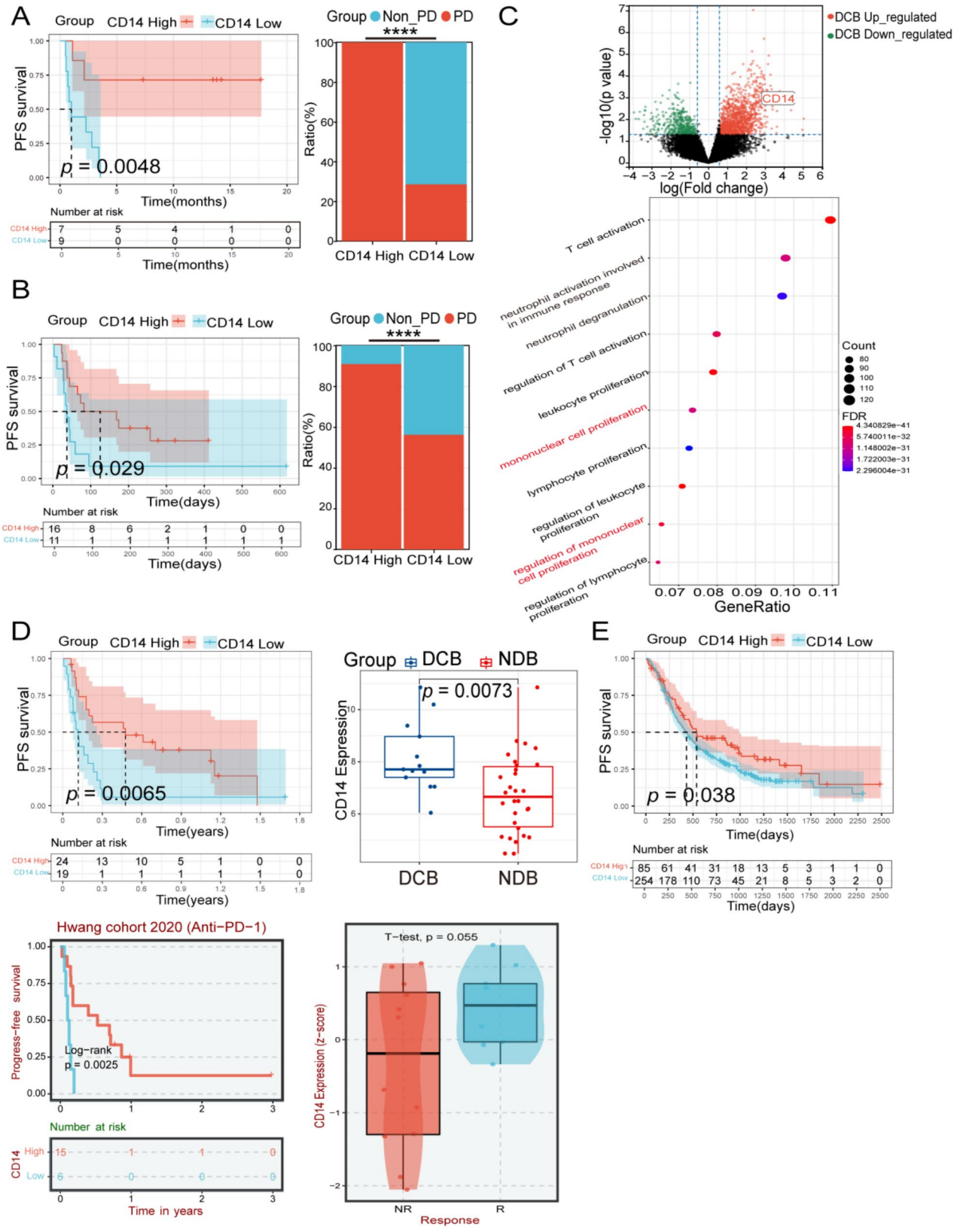

Fig. 3 (See legend on next page.)

(See figure on previous page.)

Fig. 3 Performance of *CD14* in predicting survival in GEO immunotherapy cohorts ($n = 16$, 27, and 339). (**A-B**) Kaplan-Meier curves for PFS based on *CD14* gene expression in NSCLC immunotherapy cohorts (GSE126044 and GSE135222) and comparison of PD and non-PD ratios between *CD14* high and low groups. (**C**) Differential gene analysis and functional enrichment for genes upregulated in the DCB group. (**D**) Kaplan-Meier curves for PFS based on *CD14* gene expression and comparison of *CD14* expression between DCB and NDB groups in combined and GSE136961 datasets. (**E**) Kaplan-Meier curves for PFS based on *CD14* gene expression in GSE218989 and GSE136961. (Abbreviation: GEO: Gene Expression Omnibus data base; NSCLC: non-small cell lung cancer; PFS: progression free survival; PD: progression disease; DCB: durable clinical benefit; NDB: non-durable clinical benefit. Mann-Whitney test was performed between groups)

($p < 0.05$, r = -0.26 and $p < 0.05$, r = -0.29) and counts of B cells ($p < 0.05$, r = -0.27 and $p < 0.05$, r = -0.31). Additionally, IL-17 A was positively correlated with the percentage of T cells ($p < 0.05$, $r = 0.25$) (Fig. 2B, C). sCD14 demonstrated prognostic predictive value in 21 patients with PD-L1 expression ($P < 0.05$) (Figure S2A). However, PD-L1 expression did not predict PFS, regardless of grouping method—whether dichotomized (TPS < 50% vs. TPS ≥ 50%) or categorized into three groups (TPS < 1%, TPS = 1–50%, and TPS ≥ 50%) ($P > 0.05$) (Figure S2B).

mIF and mRNA validation of CD14 in aNSCLC cohorts receiving immunotherapy

To validate the prognostic value of CD14 in predicting the efficacy of ICI therapy in NSCLC patients, we conducted mIF analysis in the CHCAMS cohort ($n = 22$) (Table S1). The analysis demonstrated that CD14 intensity was a predictor of PFS ($p < 0.05$) (Fig. 2D). Representative mIF staining of DAPI, CD14, and pan-Cytokeratin in patients with short PFS (106 days) and long PFS (511 days) was shown in Fig. 2E.

CD14 demonstrated prognostic value in both the GSE126044 ($p = 0.0048$) and GSE135222 ($p = 0.029$) datasets, patients with higher *CD14* expression associated with superior PFS and a lower percentage of patients experiencing disease progression ($p < 0.001$) (Fig. 3A, B). Differential gene analysis of the DCB and NDB groups in the GSE126044 dataset revealed that genes upregulated in the DCB group were predominantly associated with T cell activation, neutrophil activation involved in immune responses, neutrophil degranulation, leukocyte proliferation, and mononuclear cell proliferation (Fig. 3C). Combining the GSE126044 and GSE135222 datasets, *CD14* continued to show prognostic value for PFS ($p = 0.0065$) and was elevated in NDB patients ($p = 0.0073$) (Fig. 3D), the same results were also found in GSE136961 ($p < 0.05$) (Fig. 3D). Additionally, in the GSE218989 dataset, higher *CD14* expression correlated with improved PFS ($p = 0.038$) (Fig. 3E), too.

To investigate CD14 expression at both mRNA and protein levels in normal versus tumor samples, we found that CD14 mRNA levels were higher in normal samples not only in lung adenocarcinoma (LUAD) and lung squamous cell carcinoma (LUSC) but also in breast invasive carcinoma (BRCA), cholangiocarcinoma (CHOL), colon adenocarcinoma (COAD), kidney chromophobe (KICH), liver hepatocellular carcinoma (LIHC), pheochromocytoma and paraganglioma (PCPG), and rectum adenocarcinoma (READ) (Fig. 4A). In LUAD and LUSC, *CD14* expression was highest in the C6 (TGF-β dominant) subtype and lowest in the C1 (wound healing) subtype (Fig. 4B). CD14 protein levels were elevated in breast cancer, colon cancer, ovarian cancer, uterine corpus endometrial carcinoma (UCEC), and liver cancer (Fig. 4C). Additionally, CD14 protein expression was higher in normal samples of LUAD ($p = 5.61e\text{-}16$) and LUSC ($p = 5.25e\text{-}15$) (Fig. 4D).

Discussion

This study identifies pretreatment plasma sCD14 as a promising prognostic biomarker in patients with aNSCLC undergoing immunotherapy. The analysis demonstrated that sCD14, among other cytokines, shows differential expression between patients with DCB and those with NDB. Notably, sCD14 was elevated in the DCB group, indicating its potential role in predicting better responses to immunotherapy. The prognostic value of sCD14 was validated through various methods, including mIF and analysis of publicly available gene expression datasets. The consistent finding that higher sCD14 levels correlate with improved PFS across multiple datasets and cohorts underscores its robustness as a prognostic marker. This is further supported by the univariate analysis showing associations between sCD14 and PFS ($HR = 0.054$, $p < 0.001$), suggesting that patients with higher sCD14 levels before treatment are more likely to benefit from immunotherapy. While PD-L1 expression is a well-established biomarker in lung cancer immunotherapy, our study revealed that it did not significantly predict PFS in our cohort ($P > 0.05$), regardless of the grouping method. This finding suggests that sCD14 may serve as an independent prognostic biomarker beyond PD-L1 status. However, given the limited number of patients with available PD-L1 data ($n = 21$), selection bias cannot be entirely ruled out. Further validation in larger, well-balanced cohorts is warranted to confirm these findings. In conclusion, this study establishes sCD14 as a valuable prognostic biomarker for aNSCLC patients undergoing immunotherapy. Its predictive capacity, coupled with its associations with immune

cell populations and involvement in inflammatory signaling, supports its potential use in guiding therapeutic decisions and tailoring immunotherapy strategies.

In our study, we found that higher pretreatment plasma sCD14 levels were associated with better prognosis in advanced NSCLC patients undergoing immunotherapy, suggesting a potential role of sCD14 in enhancing antitumor immune responses. sCD14, a soluble co-receptor for LPS, can activate immune signaling through the TLR4 pathway, leading to increased cytokine production and immune cell activation [30–32]. As a key component of the innate immune Toll-like receptor system, the soluble form of CD14 is elevated in the serum of cancer patients, which may be associated with immune tolerance and cancer progression [33]. Previous studies have indicated that CD14 expression is linked to heightened immune infiltration and inflammatory responses in various cancers, supporting its role in shaping the tumor immune microenvironment [34]. In NSCLC, high expression of CD14 is related to increased infiltration of NK cells, classical monocytes, and intermediate monocytes, effectively predicting disease progression in IA-IB NSCLC [35, 36]. The increased tumor infiltration of $CD14^+$ cells is associated with higher staging and a greater number of positive lymph nodes at the time of surgery, serving as a biomarker for poor prognosis in early lung adenocarcinoma [37]. In NSCLC treated with immune checkpoint inhibitors, the frequency of $CD14^+$ monocytes is associated with prolonged PFS [38]. Responders to immunotherapy demonstrate higher percentages of PD-L1(+) neutrophils, PD-L1(+) CD14(+) cells, and PD-L1(+) platelets compared to pre-treatment levels [39]. Patients with a higher percentage of PD-L1 + CD14 + show shorter overall survival [40, 41]. In colorectal cancer, *CD14* is associated with high immune and stromal infiltration, and it interacts with immune checkpoints, potentially predicting the prognosis of immunotherapy [42]. In breast cancer, rectal cancer, and ovarian cancer patients, pre-treatment serum levels of sCD14 are related to the risk of recurrence and prognosis [43–46]. These results indicate that CD14 and its soluble form play an important role in immune responses and prognosis across various cancers. The correlation of sCD14 with immune cell populations, such as NK cells, adds a layer of complexity to its role in the tumor microenvironment. sCD14's positive correlation with NK cell counts ($p < 0.05$, $r = 0.24$) suggests it may enhance anti-tumor immune responses, potentially explaining the improved outcomes in patients with elevated sCD14 levels. Moreover, the observed interactions among cytokines in the protein-protein network analysis indicate a coordinated inflammatory response, with sCD14 potentially acting as a central mediator. Its involvement in key pathways, such as the MAPK signaling and cytokine production regulation, provides a mechanistic basis for its role in modulating immune responses to tumors. One possible explanation for our findings is that elevated sCD14 levels reflect a more active immune state, enhancing antigen presentation and T cell priming, which could improve response to ICIs. Additionally, sCD14 has been reported to modulate macrophage polarization and monocyte differentiation [32, 47], which may contribute to a more favorable immune landscape for ICIs. Although our study establishes a clinical association between sCD14 and immunotherapy outcomes, further in vitro and in vivo functional studies are warranted to elucidate the precise mechanisms through which sCD14 influences tumor-immune interactions. Future investigations should explore the role of sCD14 in immune cell recruitment, checkpoint regulation, and inflammatory signaling, which could provide valuable insights into its potential as a predictive biomarker for immunotherapy efficacy.

This study have several limitations. First, the retrospective design may introduce biases due to reliance on historical patient data, necessitating prospective studies to confirm sCD14's prognostic value in larger, more diverse cohorts. And we acknowledge the importance of independent prospective validation. Relevant clinical samples are currently being collected and will be incorporated into future studies to further validate our findings. Second, further research is needed to explore how sCD14 influences immune responses and treatment outcomes. Additionally, further validation in independent cohorts is necessary to ensure the generalizability of sCD14 as a prognostic biomarker. These limitations highlight the need for continued research to refine our understanding of sCD14's role in aNSCLC and its potential applications in tailoring immunotherapy strategies.

Conclusion

This study demonstrates that pretreatment plasma sCD14 level may be a prognostic indicator for aNSCLC patients undergoing immunotherapy. Elevated sCD14 levels were associated with improved PFS.

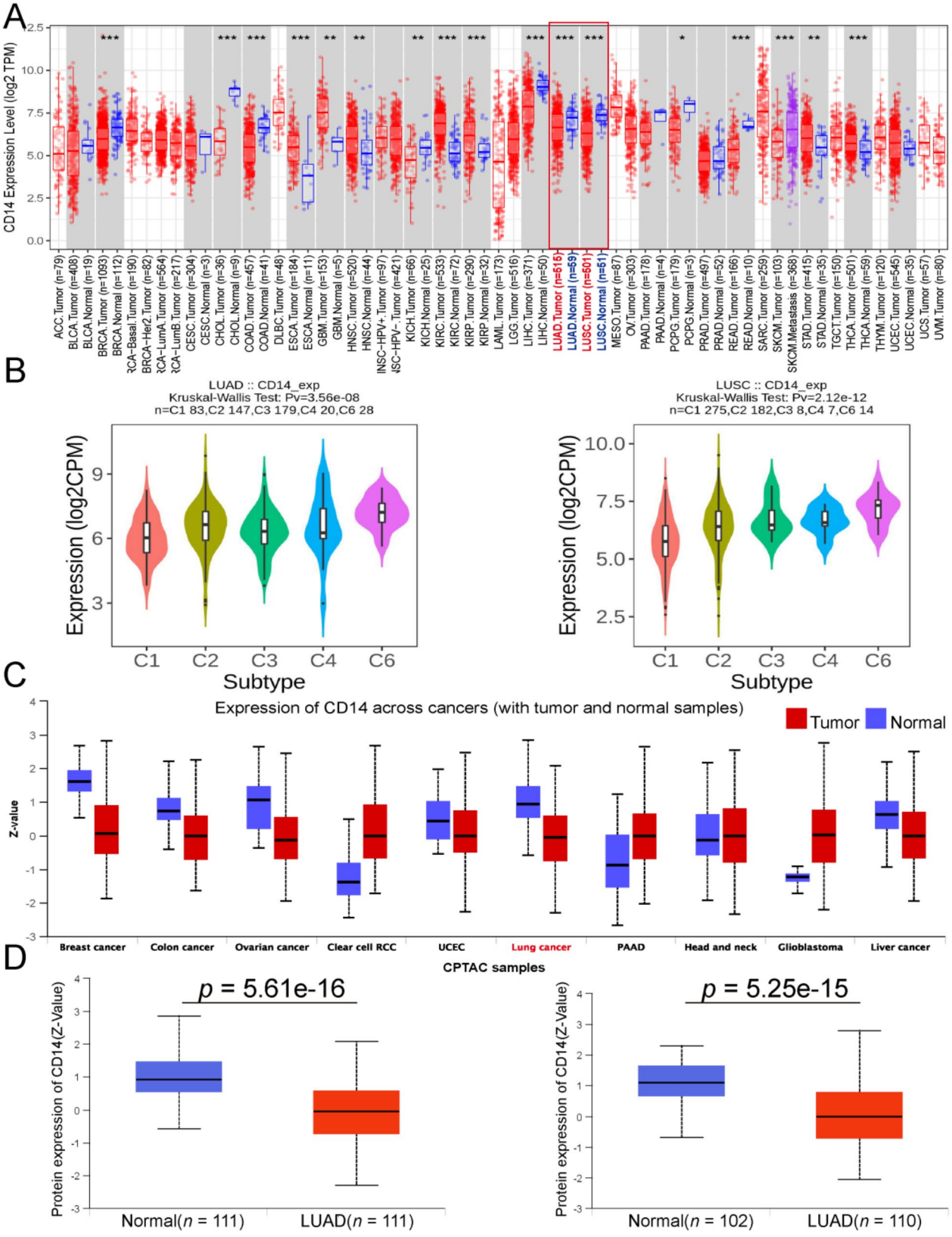

Fig. 4 CD14 gene and protein expression in the pan-cancer cohort. (**A**) Comparison of *CD14* mRNA expression between normal and tumor samples across the pan-cancer cohort. (**B**) Comparison of *CD14* expression in LUAD and LUSC subtypes. (**C**) Comparison of CD14 protein expression between normal and tumor samples in the pan-cancer cohort. (**D**) Comparison of CD14 protein expression in LUAD, LUSC, and normal samples. (Abbreviation: mRNA: messenger RNA; LUAD: lung adenocarcinoma; LUSC: lung squamous cell carcinoma. Mann-Whitney test was performed between groups)

Supplementary Information

The online version contains supplementary material available at https://doi.org/10.1186/s12885-025-14148-2.

Supplementary Material 1

Acknowledgements
Thanks to all the patients who participated in this study.

Author contributions
Liyuan Dai, Conceptualization, data curation, methodology, formal analysis, provided software, investigation, validation, visualization, writing—original draft, and writing—review & editing. Liling Huang, Resources, data curation, investigation, and writing—review & editing. Lin Li, Resources, data curation, investigation, and writing—review & editing. Le Tang, Resources, data curation, investigation, and writing—review & editing. Jiarui Yao, Resources, data curation, investigation, and writing—review & editing. Yuankai Shi, Conceptualization, funding acquisition, supervision and writing—review & editing. Xiaohong Han, Conceptualization, funding acquisition, supervision and writing—review & editing.

Funding
This work was supported by the National High Level Hospital Clinical Research Funding (2022-PUMCH-B-033), CAMS Innovation Fund for Medical Sciences under Grant (CIFMS 2021-I2M-1-003), and the Major Project of Medical Oncology Key Foundation of Cancer Hospital Chinese Academy of Medical Sciences (CICAMS-MOMP2022006).

Data availability
Data is provided within the manuscript or supplementary information files. All data included in this study are available upon request by contact with the corresponding author.

Declarations

Ethics approval and consent to participate
This study has been approved by the Ethics Committee of the National Cancer Center/National Clinical Research Center for Cancer/Cancer Hospital, Chinese Academy of Medical Sciences & Peking Union Medical College (No. 23/262–4004 and No.22/486–3688). This is a retrospective study. Plasma and tissue samples were collected after routine clinical or pathological examinations. A waiver of informed consent was granted by the institutional ethics committee. All experiments were executed according to the Declaration of Helsinki.

Consent for publication
Not Applicable.

Competing interests
The authors declare no competing interests.

Author details
[1]Department of Medical Oncology, Beijing Key Laboratory of Key Technologies for Early Clinical Trial Evaluation of Innovative Drugs for Major Diseases：National Cancer Center/National Clinical Research Center for Cancer/Cancer Hospital,, Chinese Academy of Medical Sciences & Peking Union Medical College, No. 17 Panjiayuan Nanli, Chaoyang District, Beijing 100021, China
[2]Department of Pathology, National Cancer Center/National Clinical Research Center for Cancer/Cancer Hospital, Chinese Academy of Medical Sciences & Peking Union Medical College, No. 17 Panjiayuan Nanli, Chaoyang District, Beijing 100021, China
[3]Clinical Pharmacology Research Center, Peking Union Medical College Hospital, NMPA Key Laboratory for Clinical Research and Evaluation of Drug, Beijing Key Laboratory of Key Technologies for Early Clinical Trial Evaluation of Innovative Drugs for Major Diseases, Chinese Academy of Medical Sciences & Peking Union Medical College, No.1, Shuaifuyuan, Dongcheng District, Beijing 100730, China

Received: 11 February 2025 / Accepted: 14 April 2025
Published online: 23 April 2025

References

1. Sung H, Ferlay J, Siegel RL, et al. Global Cancer statistics 2020: GLOBOCAN estimates of incidence and mortality worldwide for 36 cancers in 185 countries. CA Cancer J Clin. 2021;71:209–49. https://doi.org/10.3322/caac.21660
2. Gridelli C, Rossi A, Carbone DP, et al. Non-small-cell lung cancer. Nat Rev Dis Primers. 2015;1:15009. https://doi.org/10.1038/nrdp.2015.9
3. Borghaei H, Paz-Ares L, Horn L, et al. Nivolumab versus docetaxel in advanced nonsquamous Non-Small-Cell lung Cancer. N Engl J Med. 2015;373:1627–39. https://doi.org/10.1056/NEJMoa1507643
4. Reck M, Rodríguez-Abreu D, Robinson AG, et al. Pembrolizumab versus chemotherapy for PD-L1-Positive Non-Small-Cell lung Cancer. N Engl J Med. 2016;375:1823–33. https://doi.org/10.1056/NEJMoa1606774
5. Li CL. Song combination strategies of immunotherapy in non-small cell lung cancer: facts and challenges. Chin Med J (Engl). 2021;134:1908–19. https://doi.org/10.1097/cm9.0000000000001610
6. Michaelidou K, Agelaki S. Mavridis molecular markers related to immunosurveillance as predictive and monitoring tools in non-small cell lung cancer: recent accomplishments and future promises. Expert Rev Mol Diagn. 2020;20:335–44. https://doi.org/10.1080/14737159.2020.1724785
7. Zou W, Wolchok JD, Chen L. PD-L1 (B7-H1) and PD-1 pathway Blockade for cancer therapy: mechanisms, response biomarkers, and combinations. Sci Transl Med. 2016;8:328rv324. https://doi.org/10.1126/scitranslmed.aad7118
8. Iijima Y, Hirotsu Y, Amemiya K, et al. Very early response of Circulating tumour-derived DNA in plasma predicts efficacy of nivolumab treatment in patients with non-small cell lung cancer. Eur J Cancer. 2017;86:349–57. https://doi.org/10.1016/j.ejca.2017.09.004
9. Goldberg SB, Narayan A, Kole AJ, et al. Early assessment of lung Cancer immunotherapy response via Circulating tumor DNA. Clin Cancer Res. 2018;24:1872–80. https://doi.org/10.1158/1078-0432.Ccr-17-1341
10. Valero C, Lee M, Hoen D, et al. Pretreatment neutrophil-to-lymphocyte ratio and mutational burden as biomarkers of tumor response to immune checkpoint inhibitors. Nat Commun. 2021;12:729. https://doi.org/10.1038/s41467-021-20935-9
11. Klümper N, Saal J, Berner F, et al. C reactive protein flare predicts response to checkpoint inhibitor treatment in non-small cell lung cancer. J Immunother Cancer. 2022;10. https://doi.org/10.1136/jitc-2021-004024
12. Keegan A, Ricciuti B, Garden P, et al. Plasma IL-6 changes correlate to PD-1 inhibitor responses in NSCLC. J Immunother Cancer. 2020;8. https://doi.org/10.1136/jitc-2020-000678
13. Schalper KA, Carleton M, Zhou M, et al. Elevated serum interleukin-8 is associated with enhanced intratumor neutrophils and reduced clinical benefit of immune-checkpoint inhibitors. Nat Med. 2020;26:688–92. https://doi.org/10.1038/s41591-020-0856-x
14. Sanmamed MF, Perez-Gracia JL, Schalper KA, et al. Changes in serum interleukin-8 (IL-8) levels reflect and predict response to anti-PD-1 treatment in melanoma and non-small-cell lung cancer patients. Ann Oncol. 2017;28:1988–95. https://doi.org/10.1093/annonc/mdx190
15. Harel M, Lahav C, Jacob E, et al. Longitudinal plasma proteomic profiling of patients with non-small cell lung cancer undergoing immune checkpoint Blockade. J Immunother Cancer. 2022;10. https://doi.org/10.1136/jitc-2022-004582
16. Toi Y, Sugawara S, Sugisaka J, et al. Profiling preexisting antibodies in patients treated with Anti-PD-1 therapy for advanced Non-Small cell lung Cancer. JAMA Oncol. 2019;5:376–83. https://doi.org/10.1001/jamaoncol.2018.5860
17. Ugolini A, Zizzari IG, Ceccarelli F, et al. IgM-Rheumatoid factor confers primary resistance to anti-PD-1 immunotherapies in NSCLC patients by reducing CD137(+)T-cells. EBioMedicine. 2020;62:103098. https://doi.org/10.1016/j.ebiom.2020.103098
18. Ohue Y, Kurose K, Karasaki T, et al. Serum antibody against NY-ESO-1 and XAGE1 antigens potentially predicts clinical responses to Anti-Programmed cell Death-1 therapy in NSCLC. J Thorac Oncol. 2019;14:2071–83. https://doi.org/10.1016/j.jtho.2019.08.008
19. Zhou J, Zhao J, Jia Q, et al. Peripheral blood autoantibodies against to Tumor-Associated antigen predict clinical outcome to immune checkpoint Inhibitor-Based treatment in advanced Non-Small cell lung Cancer. Front Oncol. 2021;11:625578. https://doi.org/10.3389/fonc.2021.625578

20. Tan Q, Wang D, Yang J, et al. Autoantibody profiling identifies predictive biomarkers of response to anti-PD1 therapy in cancer patients. Theranostics. 2020;10:6399–410. https://doi.org/10.7150/thno.45816
21. Tan Q, Dai L, Wang Y, et al. Anti-PD1/PDL1 IgG subclass distribution in ten cancer types and anti-PD1 IgG4 as biomarker for the long time survival in NSCLC with anti-PD1 therapy. Cancer Immunol Immunother. 2022;71:1681–91. https://doi.org/10.1007/s00262-021-03106-z
22. Dai L, Tan Q, Li L, et al. High-Throughput antigen microarray identifies longitudinal prognostic autoantibody for chemoimmunotherapy in advanced Non-Small cell lung Cancer. Mol Cell Proteom. 2024;23:100749. https://doi.org/10.1016/j.mcpro.2024.100749
23. Liu Q, Li A, Tian Y, et al. The CXCL8-CXCR1/2 pathways in cancer. Cytokine Growth Factor Rev. 2016;31:61–71. https://doi.org/10.1016/j.cytogfr.2016.08.002
24. Bakouny Z, Choueiri TK. IL-8 and cancer prognosis on immunotherapy. Nat Med. 2020;26:650–1. https://doi.org/10.1038/s41591-020-0873-9
25. Yuen KC, Liu LF, Gupta V, et al. High systemic and tumor-associated IL-8 correlates with reduced clinical benefit of PD-L1 Blockade. Nat Med. 2020;26:693–8. https://doi.org/10.1038/s41591-020-0860-1
26. Cho JW, Hong MH, Ha SJ, et al. Genome-wide identification of differentially methylated promoters and enhancers associated with response to anti-PD-1 therapy in non-small cell lung cancer. Exp Mol Med. 2020;52:1550–63. https://doi.org/10.1038/s12276-020-00493-8
27. Jung H, Kim HS, Kim JY, et al. DNA methylation loss promotes immune evasion of tumours with high mutation and copy number load. Nat Commun. 2019;10:4278. https://doi.org/10.1038/s41467-019-12159-9
28. Kang J, Lee JH, Cha H, et al. Systematic dissection of tumor-normal single-cell ecosystems across a thousand tumors of 30 cancer types. Nat Commun. 2024;15:4067. https://doi.org/10.1038/s41467-024-48310-4
29. Hwang S, Kwon AY, Jeong JY, et al. Immune gene signatures for predicting durable clinical benefit of anti-PD-1 immunotherapy in patients with non-small cell lung cancer. Sci Rep. 2020;10:643. https://doi.org/10.1038/s41598-019-57218-9
30. Chalubinska-Fendler J, Fendler W, Spych M, et al. Lipopolysaccharide-binding protein is efficient in biodosimetry during radiotherapy of lung cancer. Biomed Rep. 2016;5:450–4. https://doi.org/10.3892/br.2016.739
31. Park BS. Lee recognition of lipopolysaccharide pattern by TLR4 complexes. Exp Mol Med. 2013;45:e66. https://doi.org/10.1038/emm.2013.97
32. Landmann R, Knopf HP, Link S, et al. Human monocyte CD14 is upregulated by lipopolysaccharide. Infect Immun. 1996;64:1762–9. https://doi.org/10.1128/iai.64.5.1762-1769.1996
33. Ciesielska A, Matyjek M. Kwiatkowska TLR4 and CD14 trafficking and its influence on LPS-induced pro-inflammatory signaling. Cell Mol Life Sci. 2021;78:1233–61. https://doi.org/10.1007/s00018-020-03656-y
34. Shive CL, Jiang W, Anthony DD, et al. Soluble CD14 is a nonspecific marker of monocyte activation. Aids. 2015;29:1263–5. https://doi.org/10.1097/qad.0000000000000735
35. Sorin M, Rezanejad M, Karimi E, et al. Single-cell Spatial landscapes of the lung tumour immune microenvironment. Nature. 2023;614:548–54. https://doi.org/10.1038/s41586-022-05672-3
36. Kapellos TS, Bonaguro L, Gemünd I, et al. Human monocyte subsets and phenotypes in major chronic inflammatory diseases. Front Immunol. 2019;10:2035. https://doi.org/10.3389/fimmu.2019.02035
37. Schenk EL, Boland JM, Withers SG, et al. Tumor microenvironment CD14(+) cells correlate with poor overall survival in patients with Early-Stage lung adenocarcinoma. Cancers (Basel). 2022;14. https://doi.org/10.3390/cancers14184501
38. Ma W, Wei S, Long S, et al. Dynamic evaluation of blood immune cells predictive of response to immune checkpoint inhibitors in NSCLC by multicolor spectrum flow cytometry. Front Immunol. 2023;14:1206631. https://doi.org/10.3389/fimmu.2023.1206631
39. Anguera G, Mulet M, Zamora C et al. Potential Role of Circulating PD-L1(+) Leukocytes as a Predictor of Response to Anti-PD-(L)1 Therapy in NSCLC Patients, Biomedicines. 2024;12. https://doi.org/10.3390/biomedicines12050958
40. Zamora Atenza C, Anguera G, Riudavets M, Melià, et al. The integration of systemic and tumor PD-L1 as a predictive biomarker of clinical outcomes in patients with advanced NSCLC treated with PD-(L)1blockade agents. Cancer Immunol Immunother. 2022;71:1823–35. https://doi.org/10.1007/s00262-021-03107-y
41. Ando K, Hamada K, Shida M, et al. A high number of PD-L1(+) CD14(+) monocytes in peripheral blood is correlated with shorter survival in patients receiving immune checkpoint inhibitors. Cancer Immunol Immunother. 2021;70:337–48. https://doi.org/10.1007/s00262-020-02686-6
42. Chen D. Wang the clinical and immune features of CD14 in colorectal cancer identified via large-scale analysis. Int Immunopharmacol. 2020;88:106966. https://doi.org/10.1016/j.intimp.2020.106966
43. He W, Tong Y, Wang Y, et al. Serum soluble CD14 is a potential prognostic indicator of recurrence of human breast invasive ductal carcinoma with Her2-enriched subtype. PLoS ONE. 2013;8:e75366. https://doi.org/10.1371/journal.pone.0075366
44. Shrout MR, Madison AA, Renna ME, et al. The gut connection: intestinal permeability as a pathway from breast cancer survivors' relationship satisfaction to inflammation across treatment. Brain Behav Immun. 2022;100:145–54. https://doi.org/10.1016/j.bbi.2021.11.012
45. Triplette M, Sigel KM, Morris A, et al. Emphysema and soluble CD14 are associated with pulmonary nodules in HIV-infected patients: implications for lung cancer screening. Aids. 2017;31:1715–20. https://doi.org/10.1097/qad.0000000000001529
46. Gadducci A, Ferdeghini M, Castellani C, et al. Serum levels of tumor necrosis factor (TNF), soluble receptors for TNF (55- and 75-kDa sTNFr), and soluble CD14 (sCD14) in epithelial ovarian cancer. Gynecol Oncol. 1995;58:184–8. https://doi.org/10.1006/gyno.1995.1207
47. Nielsen MC, Andersen MN, Rittig N, et al. The macrophage-related biomarkers sCD163 and sCD206 are released by different shedding mechanisms. J Leukoc Biol. 2019;106:1129–38. https://doi.org/10.1002/jlb.3a1218-500r

Publisher's note